/
Article / Book Information

Title	Pneumatic Soft Actuator Using Self-Excitation Based on Automatic-Jet-Switching-Structure
Authors	Kosuke Tani, Hiroyuki Nabae, Gen Endo, Koichi Suzumori
Citation	IEEE Robotics and Automation Letters (RAL), Vol. 5, Issue 3, pp. 4042-4048
Pub. date	2020, 4
Copyright	(c) 2020 IEEE. Personal use of this material is permitted. Permission from IEEE must be obtained for all other uses, in any current or future media, including reprinting/republishing this material for advertising or promotional purposes, creating new collective works, for resale or redistribution to servers or lists, or reuse of any copyrighted component of this work in other works.
DOI	https://dx.doi.org/10.1109/LRA.2020.2985622
Note	This file is author (final) version.

Pneumatic Soft Actuator Using Self-excitation Based on Automatic-Jet-Switching-Structure

Kosuke Tani[1], Hiroyuki Nabae[1], Gen Endo[1], and Koichi Suzumori[1]

Abstract—**Pneumatic pressure is a widely used power source in soft actuators as it has advantages such as simplicity of design, structure, and driving principle. However, electromagnetic valves are used for controlling pneumatic pressure, and these tend to be large and heavy, thus reducing flexibility in the main body. In this study, we devised a mechanism that generates self-excited vibration via changes in the flow path by deforming the flexible structure. Because self-excited vibration induces pressure for a certain input, actuators can be driven without using a valve in vibrating applications, which simplifies the structure of the actuator. The proposed actuator operates based on this mechanism; it has a simple structure, and thus, it can be molded easily using a 3D printer. A theoretical model of the proposed actuator was constructed, and its operating frequency was obtained via simulation. Four types of prototypes were produced, and their experimental values were compared with the theoretical values. The results of the comparison confirmed that an actuator can be designed based on the target operating frequency.**

Index Terms—**Hydraulic/Pneumatic Actuators, Additive Manufacturing, Mechanism Design, Soft Sensors and Actuators**

I. INTRODUCTION

ADVANTAGES such as simple design, structure, and driving principles, have led to pneumatic actuators being extensively used in soft actuators. Many soft actuators using air pressure have been developed to generate deformation by applying pressure to the airbag structure[1][2][3]. An electromagnetic valve is used to control pneumatic actuators and robots. Drive systems using electromagnetic valves are common; however, they tend to be heavier and larger than the pneumatic actuators and robot bodies, which impairs the flexibility of the main body and significantly weakens the advantages of soft robots in multi-degree-of-freedom systems. Although tubes can be connected based on the degrees-of-freedom without mounting a valve on the robot body, several tubes take time to connect and hinder movement. In addition, it should be noted that valve control is inevitable.

A method using self-excited vibration can be considered to simplify the control and drive system. Self-excited vibration is induced by a constant input, and it enables the integration of the control mechanism such as the actuator and the valve; further, it embeds the drive control into a
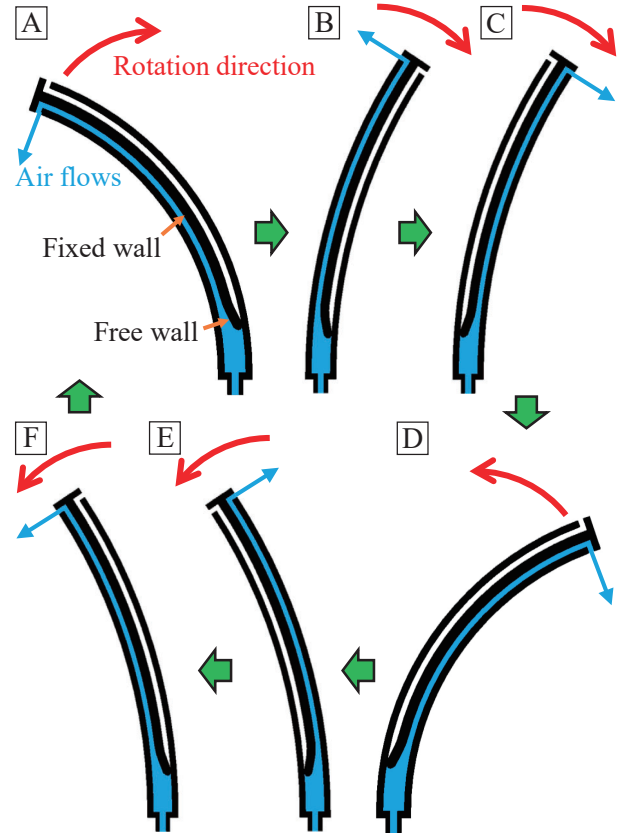
Fig. 1. Principle of operation: The internal free wall moves because of the deformation of the actuator and switching of the flow path. Because the position of the free wall is determined by the elastic force of the structural material and internal pressure, the channel does not switch at the center but experiences hysteresis.

physical phenomenon. Thus, the solenoid valve cannot be completely replaced; however these features can be used to construct a simple actuation system. This idea can be understood from the fact that various principles are applied to robots. The applications of self-excited vibration to robots include vibration induced by electrostatic force [4], excitation by link mechanism and electromagnetic motor [5][6], gravity [7][8][9], chemical reaction[10], and using deformation of bimetal with applied heat[11]. There are several examples for application of air pressure. Tsukagoshi et al. developed a valve[12] and a robot[13] that realize self-excited vibration by switching the flow path using the attractive force of a magnet. Takayama et al. developed a valve that induces self-excited vibration using the motion of a piston[14]. There is also an
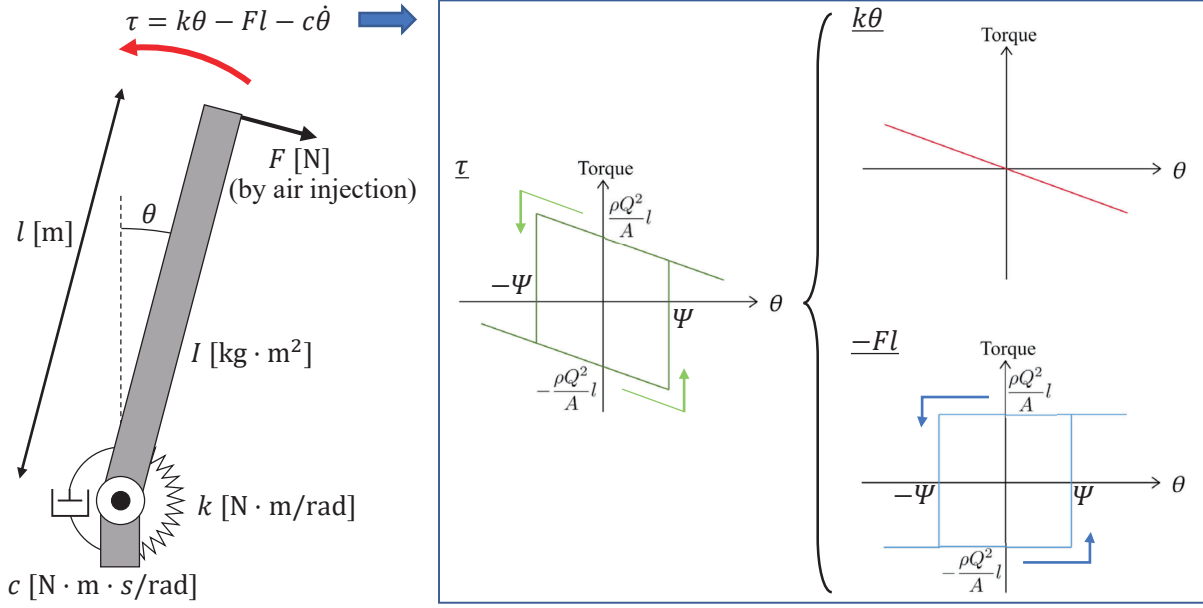
$$\tau = k\theta - Fl - c\dot{\theta}$$

Fig. 2. Model of the actuator: The body is a rigid rod of length l and receives a restoring force caused by the forces of the spring, air, and damper.

example of a mobile robot that uses self-excited vibration [15]. However, because all these robots require functional materials such as multiple members and magnets, it is difficult to achieve a completely flexible structure. To completely utilize the advantages of soft robots and actuators, it is necessary to develop a fully flexible self-excited vibration-type pneumatic actuator. A single flexible structure configuration can be used to achieve this. Furthermore, if it can be configured with a single structural member, it can be modeled by 3D printing. There are cases where soft robots are molded by 3D printing, and it confirms the superiority of using a single member[16]. This would ensure the widespread use of this system because of the simple manufacturing, which simplifies the manufacture of multi-degree-of-freedom structures and significantly expands the range of applications.

Therefore, in this study, we propose a pneumatic self-excited vibration actuator composed of a single flexible structure member that operates by switching the flow path and the thrust generated by the jet. The features of the proposed actuator are provided below.

- The proposed actuator uses the mechanism that induces self-excited vibration to perform vibrating motion only with a constant air input.
- The proposed actuator can be composed of a single member and easily manufactured by 3D printing.
- Because it operates only by injecting air, the structure and control system do not become complicated when multiple actuators are driven simultaneously.

In addition, the proposed actuator is modeled and the effects of the actuator design parameters on the operating characteristics are verified experimentally based on observations. The remainder of this this paper is organized as follows. Section 2 explains the operating principle of the proposed actuator. Section 3 discusses the theoretical model of the actuator. In

Section 4, we detail an experiment conducted on the prototype and confirm the validity of the theoretical model. Section 5 presents the conclusions of the study.

II. ACTUATOR PRINCIPLE

This section briefly explains the operating principle of this actuator.

The mechanism of inducing self-excited vibration by air has been studied in the field of fluidics[17][18]. However, many of these studies propose structures that change the flow direction [19], and it is difficult to produce a large motion as an actuator[20]. As a basic principle of actuator operation, we devised a structure wherein the air flow path is switched by structural deformation. A schematic of the actuator operation is shown in Fig. 1. The inside of the actuator is divided into two chambers by a wall provided in the center; the tip of the wall is structured to move freely. The free wall moves because of the elastic force caused by the bending of the actuator and the pressure difference between the air chambers, which changes the air flow path. In state A, the air flows through the left channel and the actuator bends to the right as it blows to the left. The flow path does not change up to state B; however, when it bends in state C, the elastic force becomes larger than the force due to the pressure difference, and the free wall moves to the opposite side. Consequently, air is ejected to the right, but it transitions to state D because of inertia. Next, D goes from E to F, A through the same process, and by repeating this, the actuator continues to vibrate.

III. THEORETICAL MODEL

In this section, we discuss a theoretical model of the actuator and consider its operating frequency.

We model the actuator as shown in Fig. 2. A continuum model is often used for accurate modeling of soft actuators;

however, in this study, it was considered as a rigid body model with a rotary joint. This is because the discussion focused on the primary mode of vibration and assumed that no external force was applied. Further, in this study, we focused on only the frequency in the motion measurement, and thus, such a simple model is believed to be sufficient. The entire actuator is considered as a rigid rod of length l [m]. It has a spring with an elastic coefficient k [N $\cdot$ m/rad] and a damper with a viscosity coefficient c [N $\cdot$ m $\cdot$ s/rad] at the center of rotation. The inclination of the bar is represented by θ [rad], and the restoring force caused by the spring follows the red plot in Fig. 2. It is assumed that air is ejected from the tip of the rod and the force generated by the air is F [N]. The rod receives a restoring force from the spring and the air, but it has hysteresis, as shown in Fig. 2 depending on the structural characteristics of the actuator. Therefore, the direction of the restoring force generated by the air changes at $\pm\Psi$.

Here, let us consider that air flows into the actuator at a flow rate of Q [m^3/s]. The force generated by the air is derived as follows. The flow path inside the actuator is considered as a two-dimensional jet model that collides with a curved surface, as shown in Fig. 3. The force $\boldsymbol{F} = (F_x, F_y)$ generated by the air on the curved surface is

Fig. 3. Pipe model: Flow path inside the actuator is considered a two-dimensional jet that collides with a curved surface.

$$\frac{\rho Q^2}{A}\left(\cos\phi - 1\right) = -F_x \tag{1}$$

$$\frac{\rho Q^2}{A}\sin\phi = -F_y \tag{2}$$

We set $\phi = \dfrac{\pi}{2}$ to obtain the force in the y direction, which is related to the torque of the rotating tube.

Fig. 4. Actuator operation simulation: A simulation was performed based on the constructed model. The figure is a block diagram used for the simulation and considers all restoring forces due to springs, dampers, and air.

$$F_y = -\frac{\rho Q^2}{A} \tag{3}$$

From this, the magnitude of the torque due to the air received by the actuator is as shown in Fig. 2.

Using these values, an actuator operation simulation was performed with MATLAB Simulink. A block diagram of the simulator is shown in Fig. 4. Here, the measured values of the prototype model described later were used for each variable; the actuator was given an initial displacement of 1 [rad]. Consequently, a vibration waveform, as shown in Fig. 5 was obtained, and it was confirmed that the vibration was sustained by the inflow of constant air. In addition, it can be confirmed that resilience is delayed for the displacement by the hysteresis characteristic. Here, the time for one step of the simulation is 10 ms.

IV. PROTOTYPE AND OPERATION EXPERIMENT OF ACTUATOR

This section first describes the prototype actuator. An operating experiment was performed on the prototype actuator to measure the operating frequency. The validity of the model is shown by comparing the measured values with the theoretical model.
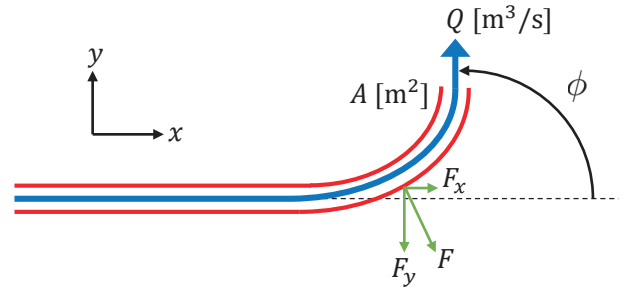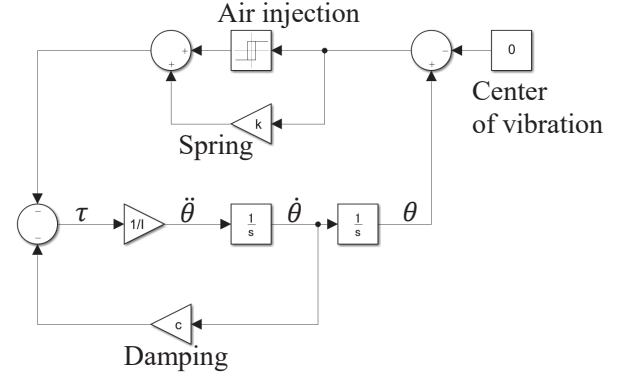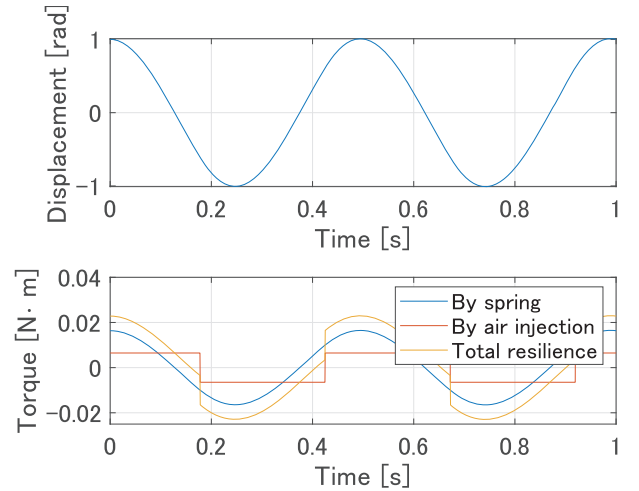

Fig. 5. Displacement and resilience of the simulated actuator: It was confirmed by simulation that the vibration continued with a constant air flow. The delay of resilience due to hysteresis can also be confirmed.

A. The prototype of actuator

The prototype actuator is shown in Fig. 6. The actuator is modeled by a 3D printer (M3DS-SA5, MITS Electronics). The main body consists of an integral part. The properties

TABLE I
PROPERTIES OF MATERIALS USED FOR 3D PRINTING

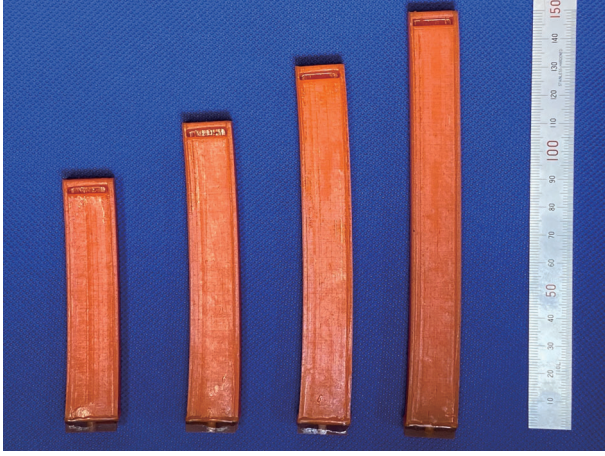|	
Elastic modulus	1 [MPa]
Tensile strength	0.9 [MPa]
Elongation at break	290 [%]
Shore A hardness	25

Fig. 6. Prototype actuators: 80, 100, 120, and 140 mm in length from the left. All operate according to the same principle. Modeled using a 3D printer.
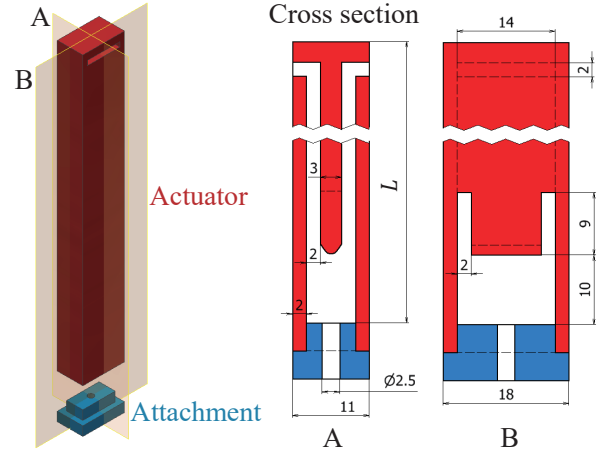

Fig. 7. Structure and dimensions of the prototype actuator: The 9 mm tip of the inner wall of the actuator is a free wall, which can move freely. With this structure, the flow path is switched, and the actuator vibrates. Air is allowed to flow into the actuator by attaching a dedicated attachment. The actuator and the attachment were bonded using ultraviolet curing resin.
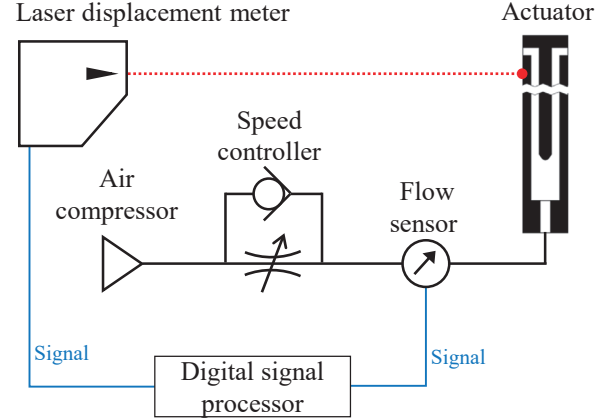

Fig. 8. System configuration of the experimental equipment: An air compressor was used as the air pressure source, and a pressure of 0.7 MPa was maintained. The air flow rate was adjusted using a speed controller and flown into the actuator. The flow rate and actuator displacement at that time were recorded.

of the materials used for printing are listed in Table I. The parameters of each actuator are listed in Table II. Because modeling revealed that the actuator length l affects the operating frequency, we designed models with a modified length.

Each parameter was measured from the actual model. l is the length of the actuator body and I is calculated from the mass and length of the body, assuming the actuator body is a cuboid structure. k was calculated by measuring the amount of deflection when deflected by its own weight. For c, the initial displacement was provided to cause free vibration, which was calculated from amplitude attenuation. Ψ is the value at which the restoring force switches in Fig. 2. This helped measure the angle at which the direction of air ejection switched by deforming the actuator. The dimensions of each part of the actuator are shown in Fig. 7; the air was introduced by connecting an attachment, as shown in figure, to the actuator. The actuator and the attachment are bonded by an ultraviolet curing resin. This resin is strong enough to not be broken by internal pressure, and there is no air leakage owing to its high sealing performance. The dimensions of the internal structure were all the same for this experiment. This experiment shows the validity of the modeling, and changes in the characteristics caused by changes in the internal structural dimensions will be considered in a future research topic.

B. Experimental setup

An experiment was conducted in which air was introduced into each actuator and the operating frequency was measured. The system configuration of the experimental equipment used is shown in Fig. 8. An air compressor was used as the air pressure source and a sufficient pressure of 0.7 MPa was

maintained. The air flow from the air compressor was adjusted with a speed controller and it was flowed into the actuator. The flow rate was changed manually during the experiment. A laser displacement meter (LKG-500, Keyence) was employed for displacing one point of the actuator. Simultaneously, the flow rate of air flowing into the actuator was measured using a flow sensor (FD-A600, Keyence). The flow rate and displacement data were recorded using a digital signal processor (DS1104, DSpace). The data sampling frequency is 10 kHz.

C. Experimental result

Air was introduced into the four models and the operating frequency was measured. Fig. 9 shows movement when air flows into Model D at 60 L/min, and it is evident that the reciprocating motion is realized by constant air flow. The displacement of one point of Model D at the representative

TABLE II
PARAMETERS OF THE PROTOTYPE ACTUATOR

Model	l [mm]^a	A [m^2]^b	I [kg · m^2]^c	k [N · m/rad]^d	c [N · m · s/rad]^e	Ψ [deg]^f
Model A	80	2.80×10^{-5}	2.58×10^{-5}	0.0391	2.22×10^{-4}	6 (at $Q = 30$ [L/min]) 10 (at $Q = 60$ [L/min])
Model B	100	2.80×10^{-5}	4.03×10^{-5}	0.0206	1.96×10^{-4}	10 (at $Q = 20$ [L/min]) 19 (at $Q = 60$ [L/min])
Model C	120	2.80×10^{-5}	5.80×10^{-5}	0.0173	1.92×10^{-4}	10 (at $Q = 20$ [L/min]) 24 (at $Q = 60$ [L/min])
Model D	140	2.80×10^{-5}	7.90×10^{-5}	0.0163	2.57×10^{-4}	21 (at $Q = 30$ [L/min]) 35 (at $Q = 60$ [L/min])

^{a}Actuator length.
^{b}Cross-sectional area of actuator flow path.
^{c}The actuator was assumed to be a rectangular parallelepiped and I is calculated from the mass and length.
^{d}It was calculated from the amount of deflection when it was bent by its own weight.
^{e}Free vibration was caused by applying the initial displacement, and the attenuation of the amplitude was measured.
^{f}The size of the hysteresis. The actuator was deformed, and the angle at which the air ejection direction switched was measured.
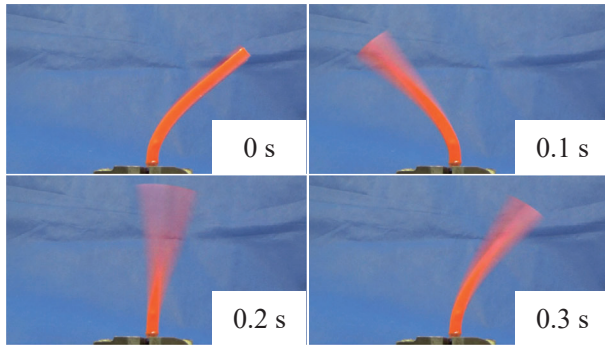

Fig. 9. Actuator operation: Performs reciprocating motion with constant air flow. The figure shows the operation when air flows into Model D at 60 L/min.
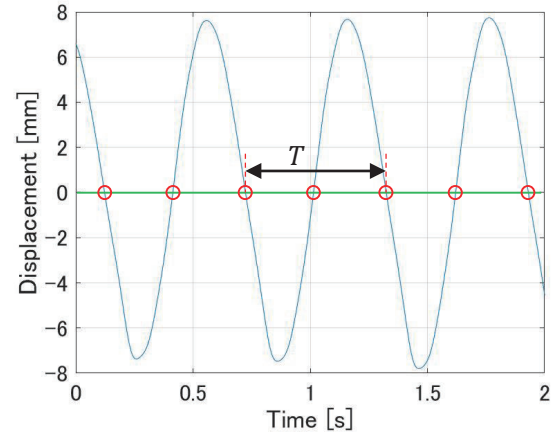

Fig. 10. Calculation of operating frequency: The figure shows the displacement of one point of the actuator recorded by the laser displacement meter. The time at which the displacement is zero is obtained, and the frequency is obtained from the time per cycle.

time obtained as a result of the experiment is shown in Fig. 10. The data are filtered by moving average with 400 samples. In the obtained waveform, the time passing through the center point was recorded and the frequency of each wave was obtained from the data. In Fig. 10, $\frac{1}{T}$ is the frequency of the waveform. The flow rate of air flowing into the actuator at each time was recorded simultaneously. The relationship between the flow rate and operating frequency obtained as a result, is shown in Fig. 11. The theoretical values derived from the model obtained in the previous section are also plotted in the same figure. These data are obtained from simulation by applying the parameters in Table II to the theoretical model.

As a result of the experiment, the value obtained from the operating frequency and the theoretical value obtained from the experiment was found to be approximately the same value. In the model with a long actuator length l, the difference between the experimental and theoretical values is large. In the theoretical model, it is assumed that the main body is a rigid rod; however, if it is large, the overall deformation becomes large, which is considered to be far from this assumption.

In the experiment, the actuator stopped operating in the region where the flow rate was approximately $40 \sim 50$ [L/min]. This is because the free wall is drawn by the force generated on the wall as per Bernoulli's theorem, as shown in Fig. 12,

and the air flows out from both channels. If the difference in the amount of air flowing out from both channels is small, the forces cancel each other, and the vibration stops. When the flow rate is smaller than this region, the force is not affected by Bernoulli's theorem. In addition, when the flow rate is larger than this region, the pressure due to the inflow of air is large; thus, the difference in the amount of air flowing out from both channels is large, and the restoring force is considered to be generated. The region where this phenomenon occurs is considered to be affected by the dimensions of the free wall, and considerations and design methods including this region will be discussed in the future.

These results indicate that the modeling method is valid. Further, it was found that operating frequency can be changed by adjusting the parameter based on the length, and the target actuator can be designed using the observations based on modeling.
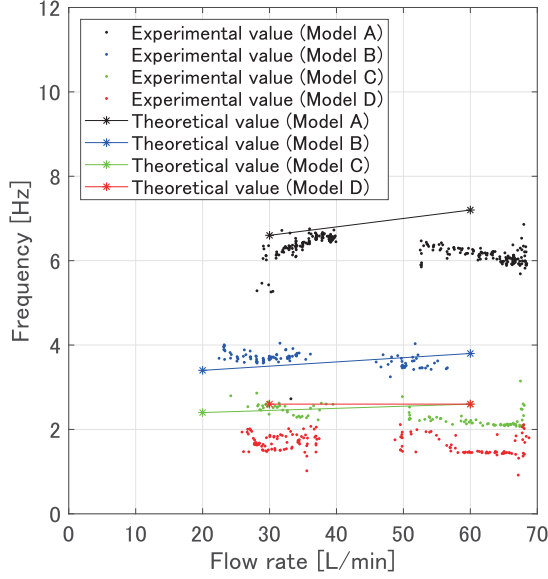
Fig. 11. Experimental result: operating frequency of the actuator obtained by the experiment and the theoretical value derived from the theoretical model are shown. It is evident that the experimental and theoretical values are almost the same. The actuator operation stopped at a flow rate of about $40 \sim 50 [\mathrm{L/min}]$; this is believed to be because the free wall was pulled by the force generated on the wall by Bernoulli's theorem.
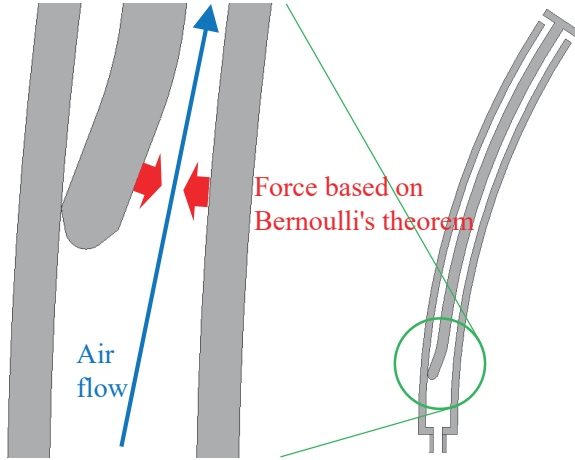

Fig. 12. Force generation by Bernoulli's theorem: Flow rate at which the actuator stopped operating was observed in the experimental results. This is because the force is generated on the wall by Bernoulli's theorem and the free wall is pulled.

V. CONCLUSIONS

In this study, we proposed a pneumatic actuator that can be molded by a 3D printer using a structure that induces self-excited vibration by bending. This actuator can induce self-excited vibration by constant air input. The operation frequency was calculated theoretically by performing operation simulations by modeling the actuator. The validity of the model was confirmed by comparing the obtained theoretical values with the experimental values of the four prototypes. In the experiment, it was confirmed that the operating frequency
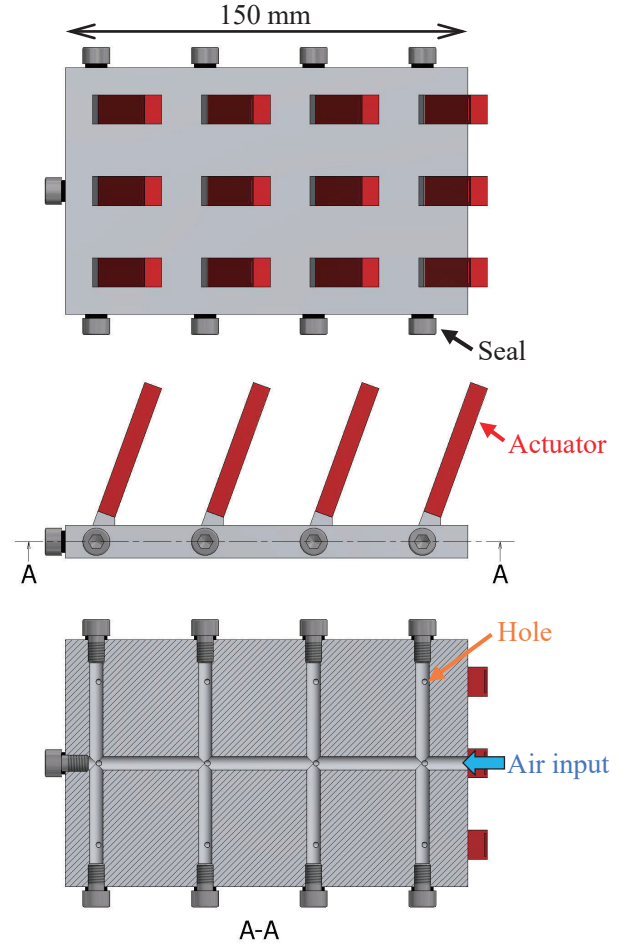

Fig. 13. Structure of multiple simultaneous driving test device: 12 actuators are bonded to the base where the flow path is arranged. By injecting air into the base, the internal structure splits the channel into 12 channels, and 12 actuators operate simultaneously.

changed with the length of the actuator, and the frequency was almost independent of the input flow rate. Further, it was also confirmed that the operation stopped within a certain flow range. These results show that an actuator with an operating frequency suited to the purpose can be designed using a theoretical model.

Future work

In this study, we focused on the operating frequency of the actuator and performed modeling and operation experiments. However, changes in the characteristics caused by changes in the internal dimensions as shown in Fig. 7 have not been studied yet; this and the effect of the structural parameters on operation will be investigated in the future.

In the experiment in this study, a stop region of $40 \sim 50 \, [\mathrm{L/min}]$ was confirmed as shown in Fig. 11. However, in practical use, it is necessary to design an actuator such that its operating frequency does not enter the stop region. Therefore, in the future, modeling will be performed considering air leakage. In addition, when considering contact with other objects, we should examine the deformation when an external force is applied using a continuum model. We believe that
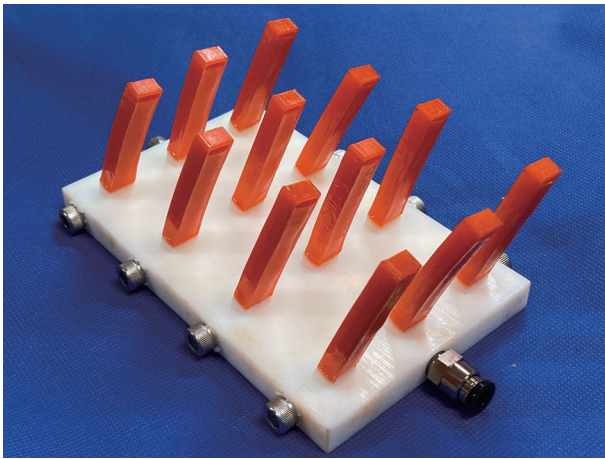
Fig. 14. Driving multiple actuators: We confirmed that multiple actuators can be driven simultaneously with a single input.

this will help expand the range of design and enable more applications.

As an application, we believe that a carrying device can be designed using many actuators, and we are currently testing its development. Fig. 13 and Fig. 14 show a structure and a photo of the test model that operates multiple actuators using a single pneumatic input and succeeds in driving multiple actuators simultaneously. 12 actuators are bonded to the base where the flow path is arranged. By injecting air into the base, the internal structure splits the channel into 12 channels, and 12 actuators operate simultaneously. It is believed that such a mechanism can be applied for moving soft objects. Further, because this actuator can easily generate an oscillatory motion, it can be applied to a leg mechanism, and we plan to consider it as a moving mechanism for a soft robot. In the future, we will study robotic applications of the actuator and discuss its usefulness.

REFERENCES

[1] D. Drotman, S. Jadhav, M. Karimi, P. deZonia, and M. T. Tolley, "3d printed soft actuators for a legged robot capable of navigating unstructured terrain," in *2017 IEEE International Conference on Robotics and Automation (ICRA)*, May 2017, pp. 5532–5538.

[2] K. Suzumori, S. Iikura, and H. Tanaka, "Development of flexible microactuator and its applications to robotic mechanisms," in *Proceedings. 1991 IEEE International Conference on Robotics and Automation*, April 1991, pp. 1622–1627 vol.2.

[3] R. Niiyama, X. Sun, C. Sung, B. An, D. Rus, and S. Kim, "Pouch motors: Printable soft actuators integrated with computational design," *Soft Robotics*, vol. 2, no. 2, pp. 59–70, 2015. [Online]. Available: https://doi.org/10.1089/soro.2014.0023

[4] H. Nabae and K. Ikeda, "Effect of elastic element on self-excited electrostatic actuator," *Sensors and Actuators A: Physical*, vol. 279, pp. 725 – 732, 2018. [Online]. Available: http://www.sciencedirect.com/science/article/pii/S092442471830709X

[5] M. NAKASHIMA, N. OHGISHI, and K. ONO, "A study on the propulsive mechanism of a double jointed fish robot utilizing self-excitation control," *JSME International Journal Series C Mechanical Systems, Machine Elements and Manufacturing*, vol. 46, no. 3, pp. 982–990, 2003.

[6] J. Ute and K. Ono, "Fast and efficient locomotion of a snake robot based on self-excitation principle," in *7th International Workshop on Advanced Motion Control. Proceedings (Cat. No.02TH8623)*, July 2002, pp. 532–539.

[7] D. Cunningham and H. H. Asada, "The winch-bot: A cable-suspended, under-actuated robot utilizing parametric self-excitation," in *2009 IEEE International Conference on Robotics and Automation*, May 2009, pp. 1844–1850.

[8] K. Ono, R. Takahashi, A. Imadu, and T. Shimada, "Self-excitation control for biped walking mechanism," in *Proceedings. 2000 IEEE/RSJ International Conference on Intelligent Robots and Systems (IROS 2000) (Cat. No.00CH37113)*, vol. 2, Oct 2000, pp. 1143–1148 vol.2.

[9] K. Ono, R. Takahashi, and T. Shimada, "Self-excited walking of a biped mechanism," *The International Journal of Robotics Research*, vol. 20, no. 12, pp. 953–966, 2001. [Online]. Available: https://doi.org/10.1177/02783640122068218

[10] S. Maeda, Y. Hara, T. Sakai, R. Yoshida, and S. Hashimoto, "Self-walking gel," *Advanced Materials*, vol. 19, no. 21, pp. 3480–3484, 2007. [Online]. Available: https://onlinelibrary.wiley.com/doi/abs/10.1002/adma.200700625

[11] T. Nemoto and A. Yamamoto, "Thermobot: A bipedal walker driven by constant heating," in *2015 IEEE/RSJ International Conference on Intelligent Robots and Systems (IROS)*, Sep. 2015, pp. 983–988.

[12] Y. Miyaki and H. Tsukagoshi, "Soft simple compact valve inducing self-excited vibration aimed for mobile robots unnecessary for electricity," in *2018 IEEE/ASME International Conference on Advanced Intelligent Mechatronics (AIM)*, July 2018, pp. 670–675.

[13] Y. Iida and H. Tsukagoshi, "Compact valve inducing self-excited vibration and its applications," *Proceedings of the 2018 JSME Conference on Robotics and Mechatronics*, vol. 2019, pp. 1P1–K10, 2019, in Japanese.

[14] T. Takayama and Y. Sumi, "Self-oscillated air flow passage changing device for bundled tube locomotive device," *Proceedings of the 2018 JSME Conference on Robotics and Mechatronics*, vol. 2016, pp. 2A2–08b2, 2016, in Japanese.

[15] D. Kim, J. I. Kim, and Y. Park, "A simple tripod mobile robot using soft membrane vibration actuators," *IEEE Robotics and Automation Letters*, vol. 4, no. 3, pp. 2289–2295, July 2019.

[16] D. B. G. J. M.Wehner, R.L.Truby and R.J.Wood, "An integrated design and fabrication strategy for entirely soft, autonomous robots," vol. 536, pp. 451–455, 2016.

[17] The Japan Fluid Power System Society, *Hydraulic and pneumatic handbook*. Ohmsha, Ltd., 1989, in Japanese.

[18] M. Harada and S. Ozaki, *Fluid particle engineering (in Japanese)*. Yokendo, 1969, in Japanese.

[19] R. Woszidlo, F. Ostermann, C. N. Nayeri, and C. O. Paschereit, "The time-resolved natural flow field of a fluidic oscillator," *Experiments in Fluids*, vol. 56, no. 6, p. 125, Jun 2015. [Online]. Available: https://doi.org/10.1007/s00348-015-1993-8

[20] J. Gregory and M. N. Tomac, "A review of fluidic oscillator development," in *43rd AIAA Fluid Dynamics Conference*, 2013, p. 2474.